Research Square

Preprints are preliminary reports that have not undergone peer review.
They should not be considered conclusive, used to inform clinical practice,
or referenced by the media as validated information.

Albumin redox-dependent pathogenic interactome driving mortality and enabling precision drug repurposing in Alcohol related liver diseases

Jaswinder Maras

jassi2param@gmail.com

Institute of Liver and Billiary Sciences https://orcid.org/0000-0003-3938-362X

Babu Mathew
Institute of Liver and Biliary Sciences

Sushimita Pandey
Institute of Liver and Biliary Sciences

Gaurav Tripathi
Institute of Liver and Biliary Sciences

Jayesh Sevak
Institute of Liver and Biliary Sciences

vasundhra Bindal
Institute of Liver and Biliary Sciences

Vipul Sharma
Institute of Liver and Biliary Sciences

Nupur Sharma
Institute of Liver and Biliary Sciences

Yash Magar
Institute of Liver and Biliary Sciences

Manisha Yadav
Institute of Liver and Biliary Sciences

Neha Sharma
Institute of Liver and Biliary Sciences

Sanju Yadav
Institute of Liver and Biliary Sciences

Shvetank Sharma
Institute of Liver and Biliary Sciences

Shiv Sarin
Institute of Liver and Biliary Sciences

Article

Keywords: Human Mercaptalbumin, Human Nonmercaptalbumin 1, Human Nonmercaptalbumin 2, Albumin modifications, Severe Alcoholic Hepatitis, Decompensated Cirrhosis, Proteomics, Metabolomics, Meta-proteomics, Bacterial peptides

Posted Date: May 8th, 2026

DOI: https://doi.org/10.21203/rs.3.rs-9331155/v1

License: This work is licensed under a Creative Commons Attribution 4.0 International License. Read Full License

Additional Declarations: There is no conflict of interest

Abstract

Background: Severe alcohol-associated hepatitis has high mortality; corticosteroids remain the only therapy. Oxidized albumin (HNA1/HNA2) accumulates, activates immune and endothelial cells, and drives inflammation leading to early mortality. The pathogenic cargos of these oxidized forms are poorly defined and albumin interactome-educated drug repurposing strategy may identify novel therapeutic targets and drug candidates.

Methods: Purified albumin redox isoforms (HMA, HNA1, HNA2) were profiled by HRMS multi-omics across controls (n=15), cirrhosis (n=50), and SAH survivors (n=30) and non-survivors (n=30). Integrated analyses identified PPIA as a key pathogenic mediator. Cyclosporine A mediated targeted inhibition of PPIA in primary neutrophils treated with SAH-derived, PPIA-enriched HNA2 was studied by functional and proteomic assays.

Results: HMA, HNA1, and HNA2 from SAH nonsurvivors harbored distinct pathogenic cargo (FC>1.5, $p<0.05$). HNA1 was enriched in inflammatory proteins, metabolites, lipids, and bacterial peptides, while HNA2 in non-survivors showed strong enrichment of hyper-inflammatory and hypoxia-associated molecules, including eicosadienoic acid, PE(P-16:0/15:1), PPIA, and bacterial peptides linked to Campylobacter concisus (FC>5, $p<0.05$), associated with TNFR1, HIF-1, and kynurenine signaling. HNA1/HNA2 signatures correlated with disease severity ($R^2>0.7$, $p<0.05$). HNA2-associated PPIA showed the highest mortality risk (HR>1.68, $p<0.05$) and emerged as the strongest predictor, guiding cyclosporine-A repurposing. Cyclosporine-A attenuated HNA2-induced neutrophil activation and oxidative stress, establishing the HNA2-PPIA axis as a therapeutically targetable axis for reduction of albumin linked inflammation in SAH patients.

Conclusion: The oxidized albumin interactome identifies PPIA as a key inflammatory mediator. Albumin interactome educated use of cyclosporine-A targets the HNA2-PPIA axis, attenuating neutrophil activation, offering a promising therapy beyond corticosteroids.

Introduction

Alcohol-related liver disease (ALD) is a major global health issue, causing widespread illness and mortality. Alcohol abuse leads to systemic inflammation, oxidative stress, metabolic problems, and multi-organ failure (1). A significant rise in the oxidative microenvironment leads to oxidative modifications of proteins, subsequently triggering immune activation and contributing to liver injury.

Human serum albumin (HSA) is produced by hepatocytes and is known to transports various endogenous and exogenous substances, including bilirubin, drugs, fatty acids, metabolites, proteins, and bacterial peptides in the circulation (2). During prolonged exposure to alcohol, albumin increasingly interacts with pathogenic biomolecules, thereby compromising its structural integrity and physiological functions. This process also triggers immune activation (5, 7) and contributes to liver dysfunction (2) (2).

In decompensated cirrhosis, albumin displays a disrupted lipidome with depletion of anti-inflammatory lipid mediators (3). In acute liver failure, albumin undergoes marked oxidative and glycosylation changes, carrying a distinct pro-inflammatory bio-molecular cargo that correlates with early mortality (2). Albumin circulates in plasma in different redox states, reflecting its critical role in keeping oxidative balance. In healthy, the majority of albumin ~ 70–80% exists in the reduced form, known as human mercaptalbumin (HMA), characterised by a free thiol group at cysteine-34 (Cys-34), which confers strong antioxidant properties. About 20–30% of albumin is HNA1, a reversibly oxidized form from mixed disulfides between Cys-34 and low-molecular-weight thiols like cysteine or glutathione. HNA2 makes up roughly 2–5% of total albumin and is an irreversibly oxidized form, with Cys-34 changed to sulfinic or sulfonic acid. This irreversible oxidation reflects prolonged exposure to oxidative stress and leads to a loss of key structural and functional properties of albumin.

In chronic alcohol exposure, the balance between redox forms of albumin shifts significantly toward oxidized variants, especially HNA2, which indicates systemic oxidative stress and altered albumin function (5). Both HNA1 and HNA2, the most extensively studied oxidized forms of albumin, have been found in previous studies to possess pro-inflammatory characteristics. In severe alcoholic hepatitis (SAH), albumin is extensively oxidized, resulting in a pro-oxidant state that affects neutrophil activity and systemic immune responses through changes in immune-regulatory functions (6). Oxidized albumin, particularly HNA1, accumulates with disease progression in cirrhosis and directly induces systemic inflammation by activating peripheral blood mononuclear cells via p38 MAPK signalling (4). In severe alcoholic hepatitis, hyperoxidized albumin especially HNA2 activates platelets via the CD36 receptor, driving inflammation, oxidative stress, and altered platelet function, thereby contributing to disease severity (5). Collectively, these studies show that HNA1 and HNA2 exhibit pro-inflammatory properties, contributing to immune cell activation and exacerbation of ALD severity. However, the precise bio-molecular cargo transported by these oxidative albumin forms, which may contribute to their pathogenicity, has yet to be identified. Additionally, their immune-stimulatory effects and correlation with early mortality remain undefined.

This study examines the bio-molecular cargo attached to HNA1 and HNA2, compared with HMA, in the plasma of SAH non-survivors. The goal is to identify harmful biomolecules; such as proteins, metabolites, lipids, and bacterial peptides bound to purified HNA1 or HNA2 that may enhance their pro-inflammatory effects and indicate ongoing liver injury, disease progression, and severity. Our findings reveal a new oxidative, albumin-bound pathogenic signature panel in SAH patients, particularly abundant in non-survivors. This panel was then used to pinpoint potential drugs for repurposing in patients with alcoholic liver disease.

Methods

Patients

The study was conducted at Institute of Liver and Biliary Sciences between April 2023 and January 2025 and included a total of 125 adult participants. The cohort included 50 patients with clinically confirmed decompensated cirrhosis, 30 survivors of severe alcoholic hepatitis (SAH), 30 non-survivors (28 days) of SAH, and 15 age- and sex-matched healthy controls. Patients with Decompensated cirrhosis was defined by the presence of one or more complications indicative of hepatic functional failure or portal hypertension, including ascites (clinically or radiologically confirmed), hepatic encephalopathy (graded I-IV per West Haven criteria), variceal gastrointestinal bleeding (confirmed via endoscopy), jaundice (serum total bilirubin > 3 mg/dL), spontaneous bacterial peritonitis (ascitic fluid neutrophil count ≥ 250/mm³), or hepatorenal syndrome (defined by International Club of Ascites criteria, REF).

Patients with compensated cirrhosis, hepatocellular carcinoma beyond Milan criteria, HIV infection, or significant extrahepatic comorbidities were excluded. SAH was diagnosed based on clinical presentation, recent onset jaundice, ongoing or recent alcohol consumption, elevated bilirubin, and AST/ALT ratio > 1.5, with further stratification into survivors and non-survivors based on 90-day clinical outcome (REF). At the time of first hospital admission, a baseline blood sample of 10 mL was collected via venipuncture from each participant using EDTA-coated vacutainers, followed by immediate plasma separation by centrifugation and storage at -80°C until further analysis. Detailed clinical, biochemical, and demographic data were recorded at admission. Laboratory investigations included complete blood count, liver and renal function tests, coagulation profile (INR), and serum sodium. Disease severity was evaluated using the Child-Turcotte-Pugh (CTP) score and the Model for End-Stage Liver Disease–Sodium (MELD-Na) score for all alcoholic patients. Where applicable, patients with acute decompensation or organ failures were further assessed using SOFA score. Written informed consent was obtained from all participants. The study protocol was approved by the Institutional Ethics Committee (IEC/2022/93/MA11) and adhered to the ethical principles.

Albumin Fractionation

EDTA plasma samples were diluted 1:100 in 0.1 M sodium phosphate and 0.3 M sodium chloride buffer at pH 6.87, then filtered through a Whatman® nylon filter discs 0.45 µm (Sigma Aldrich USA). Twenty microliters of each diluted sample were injected into a AKTA pure high-performance liquid chromatography (HPLC) system equipped with a Shodex Asahipak ES-502N 7C anion-exchange column (7.5 × 100 mm, Resonac America, Inc.). The mobile phase (A) consisted of 50 mM sodium acetate and 400 mM sodium sulfate at pH 4.85. Gradient elution was performed using the same buffer containing 10% ethanol (v/v) as mobile phase (B), applying a linear gradient from 0% to 60% B at a flow rate of 1 mL/min. Simultaneous fractions corresponding to HMA, HNA1, and HNA2 were collected during elution, aligned with their respective chromatographic peaks as previously described (6).

Untargeted Plasma Metabolomics

We used the organic phase extraction method for metabolite extraction from albumin fractions. The samples were run onto reverse-phase chromatography using C18 column (Thermo Fisher Scientific [Waltham, MA] 25003102130: 3 µm, 2.1 mm, 100 mm) using an ultra-high performance liquid chromatographic system followed by high-resolution MS. Metabolites were shown using Compound Discoverer 3.3 (Thermo Fisher Scientific). (Full protocol in Supplementary methods).

Untargeted Plasma proteomics and Meta-proteomics

100 µg equivalent protein from the albumin fractions was subjected to reduction-alkylation-digestion followed by nano-electrospray ionization and MS/MS using Q-Exactive Plus (Thermo Fisher Scientific). Proteins and Meta-proteins were identified using Protein Discoverer 2.3 (Thermo Fisher Scientific). (Full protocol in Supplementary methods)

Untargeted Plasma Lipidomics

We used the Folch method for total lipid isolation from albumin fractions. The samples were analysed using a reverse-phase chromatography using C18 column (Thermo Fisher Scientific [Waltham, MA] 25003102130: 3 µm, 2.1 mm, 100 mm) using an ultra-high performance liquid chromatographic system followed by high-resolution MS. Lipid features were identified using compound discoverer software (Thermo Fisher Scientific). (Full protocol in Supplementary methods).

Neutrophil isolation, Ex-vivo stimulation, and Flow cytometry

Peripheral blood (20 mL) was obtained from healthy adult donors and neutrophils were isolated using density gradient centrifugation. 1 × 10^6 cells/mL. neutrophils were incubated under standard culture conditions (37°C, 5% CO_2) and treated for 2 h with purified HNA2 isolated from SAH non-survivors (16 mg/mL), HNA2 plus Cyclosporin A (100 nM), or phorbol 12-myristate 13-acetate (PMA; 10 ng/mL) as a positive control. Untreated cells served as negative controls.

For surface marker staining, cells were washed with phosphate-buffered saline (PBS) and incubated with fluorochrome-conjugated monoclonal antibodies against surface markers of activation, migration, adhesion, and degranulation (Table S1) for 30 min at room temperature in the dark. Following surface staining, cells designated for intracellular cytokine detection were fixed and permeabilized using 140 µL of Cytofix/Cytoperm solution (BD Biosciences, Cat. #554714) for 10 min at room temperature. Cells were then washed with 1× Perm/Wash buffer (BD Biosciences) and incubated with fluorochrome-conjugated antibodies against intracellular targets (Table S1) for 20 min at room temperature in the dark.

After staining, cells were washed, resuspended in PBS, and subjected to single-color compensation controls. Data acquisition was performed on a BD FACSAria™ Fusion II flow cytometer (BD Biosciences).

A minimum of 100,000 events per sample were collected using identical instrument settings across all experimental runs.

Flow cytometric data were analyzed using FlowJo software version 10.8 (BD Biosciences). Quality control steps included time-based gating, exclusion of debris, doublet discrimination (FSC-A vs. FSC-H), and live/dead cell discrimination. Neutrophils were identified based on forward- and side-scatter properties and CD16/CD66b expression. Gating strategies were standardized and applied uniformly to all samples to ensure consistency and reproducibility.

Statistical analysis

Statistical analysis was performed using GraphPad Prism version 6 and SPSS version 20; $p < 0.05$ using Benjamini-Hochberg correction were considered significant. Results are shown as mean and SD unless indicated otherwise. Paired (two-tailed) Student's t test and the Mann-Whitney U test were performed for two-groups comparison. For comparison among more than two groups, one-way ANOVA and the Kruskal-Wallis test was performed. All correlations were performed using Spearman correlation analysis, and $r2 > 0.5$ and $p < 0.05$ were considered significant. For proteomics and metabolomics, Perseus and Metaboanalyst 5.0 were used; data were log normalized and subjected to Pareto scaling and further subjected to multivariate projection analyses including principal-component analysis, PLS-DA, Random Forest analysis. Pathway enrichment patterns were identified for metabolites and proteins individually using Metabolanalyst and EnrichR. Integration and correlation plots were made using Rstudio (R version 4.0.1).

Results

Oxidative stress driven remodeling of albumin redox isoforms in severe alcohol-associated hepatitis

Severe alcohol-associated hepatitis (SAH) leads to persistent inflammation and oxidative stress, altering circulating albumin's redox state and increases the conversion of Native mercapta-albumin (HMA) into reversible oxidized forms: HNA1 and irreversible oxidation form HNA2 with strong pro-inflammatory and pro-oxidant effects (4, 5, 7).

Previously, we found that albumin carries various pro-inflammatory and pro-oxidant molecules in acute liver failure (3). However, the biomolecular cargo of specific pathological albumin isoforms in SAH remains unreported. This study identifies pathogenic signatures linked to oxidised albumin, showing that HNA2 drives inflammation and could be a treatment target. The oxidised albumin interaction map also suggests possibilities for drug repurposing in alcoholic liver diseases (Fig. 1A).

Plasma samples were collected from four groups: healthy controls (n = 15), decompensated cirrhosis patients (n = 50), SAH survivors (n = 30), and non-survivors (n = 30). Albumin redox isoforms (HMA, HNA1, HNA2) were separated via anion-exchange chromatography and confirmed with proteomics

analysis. Multi-omics profiling of each fraction identified albumin-bound biomolecular signatures, prioritising those in SAH non-survivors by fold change, AUC, significance, and Random Forest scores as pathogenic candidates for HNA1 and HNA2. The top HNA2-associated molecule tied to 30-day mortality was selected for functional validation, and its inhibition tested with neutrophil assays to assess inflammation and oxidative responses. These findings point to HNA2-linked molecules as mediators of inflammation and early mortality in SAH, presenting them as potential therapeutic targets.

Pathogenic remodelling of the bio-molecular cargo bound to reduced albumin (HMA) in SAH non-survivors

To determine whether the pathological milieu of severe alcohol-associated hepatitis alters the biomolecular cargo carried by reduced albumin, HMA fractions were isolated and subjected to multi-omics analysis across healthy controls, patients with decompensated cirrhosis, SAH survivors, and SAH non-survivors (Fig. 2A).

Native albumin (HMA) multi-omics profile is distinct for SAH non-survivors, indicating a disease and outcome specific interactome (Fig. 2B) which was significantly enriched with pro-inflammatory and pro-oxidant species (Fig. 2C).

HMA fractions from healthy individuals showed relative enrichment of anti-inflammatory and homeostatic macromolecules ($p < 0.05$), though HMA from SAH non-survivors showed significant accumulation of metabolites; L-cystathionine (FC > 5.7), N,N-dimethylhistidine (FC > 3.3), Enterolactone (FC > 2.5) and others, consistent with perturbed sulphur amino acid metabolism and oxidative stress ($p < 0.05$, Supplementary Table 4). Lipid profiling identified enrichment of pro-inflammatory and membrane-disruptive species, including Cer(t18:1(6OH)/24:0(2OH)) (FC > 3.4) and MGMG(18:2(9Z,12Z)/0:0) (FC > 2.7, and others Supplementary Table 2).

SAH non-survivors HMA proteomic analysis further revealed preferential binding of inflammatory and stress-response proteins, including protein arginine methyltransferase 1 (PRMT1; FC > 11), dedicator of cytokinesis 6 (DOCK6; FC > 8.4), neurotrophin 3 (NTF3; FC > 7.4), and NOD-like receptor X1 (NLRX1; FC > 6.9, and others $p < 0.05$, Supplementary Table 5). Notably, bacterial meta-proteomic signatures were also markedly enriched, indicating enhanced microbial translocation or impaired clearance. These included peptides mapping to *Ehrlichia chaffeensis* (FC > 10.9), *Staphylococcus aureus* (FC > 8.2), *Legionella pneumophila* (FC > 6.8), and *Bacteroides fragilis* (FC > 6.7, $p < 0.05$, and others Supplementary Table 3).

HMA bound cargo in non-survivor were linked to inflammatory and metabolic exhaustion–associated pathways (Fig. 2D). These included glyoxylate and dicarboxylate metabolism, ethanol-induced histone modification effects, mitochondrial immune signaling, glycosphingolipid metabolism, and interleukin-23 signaling ($p < 0.05$). Together, these results show that HMA in SAH non-survivors contains harmful inflammatory, oxidative, and metabolic molecules despite its reduced redox state. This altered composition likely leads to immune dysregulation, tissue damage, and poor clinical outcomes, indicating that albumin dysfunction in SAH is not limited to redox changes.

HNA1 carries a distinct pro-inflammatory and microbial-enriched bio-molecular cargo in SAH non-survivors

To characterise the molecular landscape linked to reversibly oxidised albumin, HNA1 fractions were purified by anion-exchange chromatography and analysed with UHPLC-HRMS multi-omics profiling. Metabolites, lipids, host proteins, and bacterial peptides bound to HNA1 were examined for SAH non-survivors and compared with survivors, decompensated cirrhotics, and healthy controls (Fig. 3A).

HNA1-associated multi-omics dataset showed clear segregation of SAH non-survivors from healthy individuals and disease controls, indicating outcome-specific remodeling of the HNA1 interactome (Fig. 3B). Heatmap analysis of the top 20 biomolecules by fold change and significance shows that the HNA1 fraction in SAH non-survivors is enriched with pathogenic cargo.

Metabolomic profiling showed significant accumulation of bioactive metabolites associated with mitochondrial stress and immune activation in SAH non-survivor HNA1, including Elaidic carnitine (FC > 5.9), heptanoylcarnitine (FC > 4.3), histidine (FC > 3.8, and others Supplementary Table 8). Lipidomics showed enrichment of potent inflammatory and eicosanoid-related species, including leukotriene C4 (FC > 3.1), triglyceride TG(17:2/20:5/20:5) (FC > 7.9), ether phosphatidylcholine PC(O-14:0/18:2) (FC > 7.5), tetranor-prostaglandin E1 (FC > 6.5, and others), highlighting a strong pro-inflammatory lipid signature bound to HNA1 in SAH ($p < 0.05$, Supplementary Table 6).

HNA1 of SAH Non-survivors showed significant enrichment of immune-regulatory and stress-response proteins; included ring finger protein 157 (RNF157; FC > 10.1), mitogen-activated protein kinase 1 (MAP4K1; FC > 8.0), tachykinin receptor 1 (TACR1; FC > 7.0), and interferon alpha-1 (IFNA1; FC > 6.6) and others, Supplementary Table 9.

Notably, HNA1 fractions from SAH non-survivors exhibited substantial enrichment of bacterial meta-proteomic signatures, indicating enhanced microbial translocation or impaired immune clearance. These included peptides mapping to *Bacillus cereus* (FC > 6.3), *Listeria monocytogenes* (FC > 6.1), *Clostridium perfringens* (FC > 5.9), *Klebsiella pneumoniae* (FC > 5.6), and *Salmonella typhi* (FC > 5.3) and others, suggesting that HNA1 serves as a circulating scaffold for pathogen-associated molecular components in advanced disease (Fig. 3C, Supplementary Table 7).

Pathway enrichment analysis in SAH non-survivors showed increased immune-inflammatory and cell death signaling (Fig. 3D), including B-cell activation, necroptosis, interferon signaling, prostaglandin biosynthesis, and TRP channel activation ($p < 0.05$). These pathways indicate immune hyper-activation, stress adaptation, and amplified inflammation.Together our findings suggest that HNA1 in SAH non-survivors contains a pathogenic mix of inflammatory metabolites, lipids, immune proteins, and microbial products, likely driving immune disruption, metabolic exhaustion, and poor outcomes, implicating HNA1 in severe alcohol-associated hepatitis pathogenesis.

HNA2 harbours hyper-inflammatory and hypoxia-associated bio-molecular cargo in SAH non-survivors

HNA2 (Human non-mercaptalbumin-2), the irreversibly oxidized albumin isoform, has previously been shown to correlate positively with early mortality in chronic liver disease (8). To elucidate the mechanistic basis of this association, HNA2 was fractionated by anion-exchange chromatography and subjected to comprehensive UHPLC-HRMS–based multi-omics profiling. Metabolites, lipids, host proteins, and bacterial peptides bound to HNA2 were analyzed across healthy controls, patients with decompensated cirrhosis, SAH survivors, and SAH non-survivors (Fig. 4A). HNA2-associated multi-omics dataset demonstrated robust segregation of SAH non-survivors from all other clinical groups, indicating profound outcome-specific remodeling of the HNA2 interactome (Fig. 4B). A comprehensive heat-map highlighted the most discriminatory HNA2-bound biomolecules across macromolecular classes. Metabolomic analysis revealed marked enrichment of hyper-inflammatory, bile acid–derived, and bacterial-associated metabolites in the HNA2 fraction from SAH non-survivors. Prominent species included eicosadienoic acid (FC > 5.3), deoxycholic acid (FC > 3.9), muramic acid (FC > 2.3), and chenodeoxycholyl-arginine (FC > 2.3) and others, collectively reflecting dysregulated lipid signaling, bile acid metabolism, and microbial product accumulation (Supplementary Table 12).

Consistently, lipidomic profiling demonstrated significant enrichment of inflammatory and membrane-remodeling lipid species bound to HNA2 in SAH non-survivors. These included plasmalogen PE(P-16:0/15:1) (FC > 5.4), 4,7,10,13-docosatetraenoic acid (FC > 4.5), PC(12:0/18:1, FC > 4.5), and phosphatidic acid PA(20:1/0:0; FC > 3.6, and others), indicating enhanced pro-inflammatory lipid signaling and altered cellular stress responses (Supplementary Table 10).

Proteomic analysis further revealed over-representation of proteins implicated in chronic immune activation, hypoxia sensing, and stress adaptation. Key HNA2-associated proteins in SAH non-survivors included signal peptide peptidase-like 2B (SPPL2B; FC > 8.0), peptidyl-prolyl isomerase A (PPIA; FC > 5.0), serine protease 33 (PRSS33; FC > 4.2), sialic acid-binding Ig-like lectin 10 (SIGLEC10; FC > 3.6), and C-type lectin domain family 4 member D (CLEC4D; FC > 3.5, and others), consistent with sustained innate immune activation and impaired resolution of inflammation (Supplementary Table 13).

In parallel, HNA2 fractions from SAH non-survivors showed substantial enrichment of bacterial meta-proteins, suggestive of gut barrier dysfunction and systemic microbial exposure. Enriched taxa included *Campylobacter concisus* (FC > 6.7), *Pseudomonas aeruginosa* (FC > 3.6), *Clostridium perfringens* (FC > 2.7), *Salmonella paratyphi* (FC > 2.2), and *Streptococcus pyogenes* M6 (FC > 2.2) and others, indicating pronounced microbial translocation and immune engagement (Supplementary Table 11, Fig. 4C).

Pathway enrichment analysis of HNA2-bound biomolecules in SAH non-survivors revealed a significant presence of inflammation and hypoxia-related signaling networks, such as the kynurenine pathway, arachidonic acid metabolism, TNFR1, HIF-1, and cellular responses to hypoxia ($p < 0.05$, Fig. 4D). These results point to ongoing inflammation, hypoxic stress, and immune-metabolic exhaustion. Collectively,

HNA2 in SAH non-survivors carries a harmful cargo enriched with inflammatory, hypoxia-responsive, and pathogenic peptides, marking it as both an indicator of disease severity and a potential mediator of immune dysfunction and poor clinical outcomes in severe alcohol-associated hepatitis.

HNA1 and HNA2 selectively associate with therapeutically tractable bio-molecular networks in SAH non-survivors

To assess the pathological importance of oxidized albumin in severe alcohol-associated hepatitis (SAH), we examined HNA1 and HNA2, mapping their biomolecular cargo to functional pathways. We prioritised binders with a fold change > 1.5 compared to HMA and $p < 0.05$. Among SAH non-survivors, HNA1 had 68 enriched biomolecules; 36 novel and 32 previously linked to disease. HNA2 included 87 enriched binders, with 35 new and 52 known disease-associated molecules (Fig. 5A), revealing a broader pathogenic interactome for HNA2. Pearson correlation analysis using strict criteria (FC > 1.5, AUC > 0.95, $p < 0.05$) showed that most biomolecules enriched in the HNA1 fraction from SAH non-survivors were strongly correlated with HNA1 abundance ($R^2>0.7$), indicating a close link between albumin oxidation and pathological cargo (Supplementary Fig. 1). Functional annotation revealed that HNA1-associated biomolecules are mainly involved in inflammatory signaling and oxidative stress, as well as metabolic disorder, fibrosis, retinoid metabolism, apoptosis, necroptosis, gut dysbiosis, proteostasis, tumorigenesis, and anti-inflammatory responses (Fig. 5B). These findings suggest HNA1 is a selective carrier promoting inflammation and redox imbalance in SAH non-survivors. Potential therapeutic targets among HNA1-associated biomolecules were identified (Fig. 5C).

A parallel analysis of the HNA2 fraction from SAH non-survivors demonstrated even stronger and more uniform associations between albumin oxidation and cargo enrichment. All differentially enriched HNA2-associated biomolecules exhibited robust correlations with HNA2 abundance ($R^2>0.7$) (Supplementary Fig. 2). Functional categorization revealed 57 biomolecules involved in inflammatory signaling and 15 associated with oxidative stress, along with additional molecules implicated in apoptosis, fibrosis, metabolic stress, gut dysbiosis, oxidative stress responses, and anti-inflammatory signaling (Fig. 5D). As with HNA1, systematic drug target mapping identified multiple inhibitors and therapeutic agents capable of modulating the HNA2-associated pathogenic cargo (Fig. 5E).

Collectively, these analyses demonstrate that HNA1 and HNA2 in SAH non-survivors are not passive oxidation products but are tightly linked to coordinated networks of inflammatory, oxidative, and tissue-damaging biomolecules. The strong correlation between oxidized albumin isoforms and their deleterious cargo, together with the identification of therapeutic targets, supports the concept of albumin detoxification as a viable therapeutic strategy aimed at disrupting pathogenic albumin cargo interactions and mitigating disease severity in SAH.

Integrated machine learning and survival modelling identifies a core set of highly pathogenic HNA1 and HNA2 bound bio-molecules in SAH non-survivors

To delineate the most pathogenic macromolecules associated with oxidized albumin in SAH, we performed a multi-layered biomarker prioritization strategy integrating statistical significance, fold change, area under the curve (AUC), Random Forest mean decrease in accuracy (MDA), multivariate AUC modelling, Cox proportional hazards regression, and clinical correlation analyses (Fig. 6A). This approach enabled identification of the top five HNA1 and HNA2 bound bio-molecules in SAH non-survivors with the strongest discriminatory and prognostic performance. Among HNA1 associated bio-molecules, the top five candidates exhibiting AUC > 0.9 were ring finger protein 157 (FC > 10.12), forkhead box S1 (FC > 8.94), mitogen-activated protein kinase1 (MAP4K1; FC > 8.01), TG(17:2(9Z,12Z)/20:5(5Z,8Z,11Z,14Z,17Z)/20:5(5Z,8Z,11Z,14Z,17Z))[iso3](FC > 7.9), and PC(O-14:0/18:2(9Z,12Z; FC = 7.55, $p < 0.05$) respectively.

Among HNA2 associated bio-molecules, the top five discriminative binders (AUC > 0.9) comprised signal peptide peptidase–like 2B (FC > 7.99), a bacterial peptide (NANKAELTYCDGEK) derived from UDP-3-O-acylglucosamine N-acyltransferase (LpxD) of Campylobacter concisus (FC > 6.73), PE(P-16:0/15:1(9Z); FC = 5.41), Eicosadienoic acid (FC = 5.29), and peptidylprolyl isomerase A (PPIA; FC > 4.98,). Probability of detection (POD) analysis demonstrated that all top five HNA1 bound macromolecules achieved detection probabilities exceeding 80% (AUC > 80), while the top five HNA2 bound macromolecules exhibited POD values greater than 88%, confirming their robust discriminatory performance ($p < 0.05$) (Fig. 6B).

Prioritized biomolecules showed significant associations with liver disease severity scores (MELD-Na, Maddrey's Discriminant Function, ALBI, PALBI), albumin modification markers, organ function tests, blood counts, and electrolyte levels (Fig. 6C), highlighting a close link between oxidized albumin cargo and systemic dysfunction.

Receiver operating characteristic analysis showed that the top five HNA2-associated biomolecules had the highest AUROC values for identifying SAH non-survivors, highlighting their prognostic value (Fig. 6D). Cox proportional hazards modelling confirmed these as significant mortality predictors with hazard ratios above one (Fig. 6E); PPIA was the strongest predictor (HR > 1.68), followed by Eicosadienoic acid (HR > 1.30).

PPIA is a well-studied pro-inflammatory protein with a pharmacological inhibitor, Cyclosporin A, currently undergoing clinical trials (9) (Fig. 6F). These findings identify key oxidized albumin-bound biomolecules that differentiate SAH non-survivors, predict outcomes, and highlight potential therapeutic targets.

Cyclosporin A ameliorates HNA2 induces a PPIA-dependent pro-inflammatory and pro-oxidant activation in primary human neutrophils.

HNA2 directly induce immune activation including neutrophils, platelets and others (4, 5, 7). To evaluate the pathogenic significance of the PPIA-HNA2 axis in SAH non-survivors, we tested if SAH plasma-derived HNA2 directly affects neutrophil activation and whether Cyclosporin A, a PPIA inhibitor, reduces these effects. Healthy donor neutrophils were exposed to HNA2 from SAH Non-survivor (at patients'

concentration), PMA (positive control), or SAH HNA2 with cyclosporin A, and was further analyzed by flow cytometry and proteomic profiling (Fig. 7A).

Cyclosporin A markedly inhibited SAH-HNA2-mediated neutrophil activation, migration, degranulation, and adhesion/migration phenotypes ($CD16^+CD66b^+$ subsets; $p < 0.05$, Fig. 7C). It also significantly reduced HNA2 or PMA-induced $CD16^+CD66b^+TNF\alpha^+$ neutrophils and increased anti-inflammatory IL-10 expression in $CD16^+CD66b^+IL\text{-}10^+$ neutrophils ($p < 0.05$, Fig. 7C).

Peptidylprolyl isomerase A (PPIA), or cyclophilin A, acts as a pro-inflammatory mediator, activating immune responses through pathways such as NFAT, Akt, NF-κB, ERK1/2, and JNK. Immune cells release PPIA in response to injury and oxidative stress. When PPIA binds CD147 and CD18 receptors, it is internalised and forms the PPIA-CALM1-PPP3CA complex, which triggers transcriptional programs driven by NFAT, Akt, NF-κB, ERK1/2, and JNK (9). Activation of these pathways culminates in robust induction and secretion of pro-inflammatory mediators, including TNFα, IFNγ, IL-1β, IL-5, IL-6, IL-8, CXCL3, MMP9, and MCP-1, thereby amplifying inflammatory signaling in a paracrine manner (Fig. 7D). Proteins involved in neutrophil degranulation and phagocytosis such as GCA, CAMP, MPO, CTSG, PRTN3, LTF, DEFA3, MMP8, and AZU1 were significantly upregulated ($FC > 2$, $p < 0.05$) following HNA2 or PMA treatment which got significantly reduced upon cyclosporin A treatment respectively (Fig. 7E). Neutrophil proteins mediating adhesion, migration, NETosis, and cytoskeletal remodeling (S100A8, S100A9, FLNA, CEACAM6, S100A4, CALM1, CEACAM8, CD63, S100A6, and VIM) were also ameliorated post treatment with cyclosporin A.

HNA2 or PMA stimulation significantly induced proteins associated with leukotriene/eicosanoid-driven chemotaxis and inflammation LTA4H, RETN, FABP5, ALOX5AP, and THBS1, and was significantly attenuated by cyclosporin A. Components of the oxidative burst machinery (CYBA, NCF1, CYBB, NCF2, GSTO1, and CAT) were significantly elevated by HNA2 or PMA and significantly reduced with cyclosporin A treatment. Conversely, antioxidant proteins PRDX2, PRDX5, PRDX6, and P4HB exhibited significantly decreased abundance following HNA2 or PMA stimulation and were significantly restored by cyclosporin A. Anti-inflammatory proteins, including A2M, ANXA1, ANXA3, and ANXA4, displayed a similar restorative pattern with cyclosporin A (Fig. 7E) (Supplementary Fig. 3).

Given that PPIA appeared as the strongest mortality predictor among HNA2-bound biomolecules, we specifically examined downstream components of PPIA signaling. Proteins involved in PPIA-associated signaling cascades CALM1, FKBP1A, KDM7A, MAPK14, TRAF2, HDAC7, HSPA1A, HSP90AB1, and MAP2K2 were significantly increased following HNA2 or PMA treatment and significantly reduced in the presence of Cyclosporin A (Fig. 7F).

These findings show that SAH-derived HNA2 triggers PPIA-dependent neutrophil activation, increasing degranulation, migration, oxidative burst, eicosanoid signaling, and inflammatory cytokine production while reducing antioxidant and anti-inflammatory responses. Inhibiting PPIA with cyclosporin A reverses these effects, highlighting the therapeutic potential of targeting excessive PPIA in severe alcohol-associated hepatitis.

Discussion

Severe alcohol-associated hepatitis (SAH) is characterized by overwhelming systemic inflammation, oxidative stress, immune dysregulation, and high short-term mortality (10), yet the mechanistic drivers linking these processes to clinical outcomes remain incompletely defined. Albumin, the most abundant circulating protein, has traditionally been viewed as a passive marker of disease severity and nutritional status (11). Increasing evidence, however, indicates that albumin undergoes extensive structural and functional remodeling under conditions of oxidative stress and inflammation, acquiring bioactive properties that may actively shape disease pathogenesis (12). Our previous study revealed that albumin-bound cargo in ALF non-survivors is predominantly enriched with inflammatory and pathological bio-molecules (2). In this study, we provide an isoform-resolved, systems-level characterization of albumin-bound bio-molecular cargo in SAH and demonstrate that oxidized albumin particularly hyperoxidized albumin (HNA2) serves as a pathogenic scaffold that concentrates inflammatory, oxidative, microbial, and hypoxia-associated molecules, thereby amplifying immune dysfunction and contributing to early mortality. Importantly, we identify a therapeutically tractable HNA2-PPIA complex and demonstrate its functional relevance using primary human neutrophils, establishing oxidized albumin not only as a biomarker but also as a mechanistic driver and therapeutic target in SAH. Previous studies have shown that oxidized albumin isoforms increase progressively with worsening liver disease and are strongly associated with adverse clinical outcomes (13).

HNA1 and HNA2 have been demonstrated to exert direct pro-inflammatory and pro-oxidant effects in cirrhosis and acute-on-chronic liver failure (4, 5). Additionally, oxidized albumin has been linked to impaired immune function in alcohol-related liver disease (7). Our data extend these observations by showing that oxidation state alone does not fully capture albumin dysfunction; rather, each isoform harbours a distinct and biologically meaningful interactome that determines its pathogenic potential. This concept aligns with emerging paradigms in plasma proteostasis, wherein carrier proteins act as dynamic reservoirs for bioactive molecules whose composition shifts with disease context (14).

A key finding of our study is that even reduced albumin (HMA) from SAH non-survivors carries a pathogenic cargo enriched in inflammatory metabolites, lipids, immune proteins, and bacterial peptides. This observation suggests that albumin dysfunction in SAH precedes or occurs independently of irreversible oxidation, likely reflecting saturation of albumin's detoxification capacity in the setting of overwhelming systemic inflammation. Prior work has shown that albumin from patients with advanced cirrhosis exhibits impaired ligand-binding and antioxidant capacity despite preserved concentration, supporting the notion of "qualitative albumin deficiency" (15). Our results provide mechanistic depth to this concept by demonstrating that HMA itself becomes a carrier of deleterious molecules, including PRMT1, NLRX1, and bacterial peptides, which have been individually implicated in innate immune activation, mitochondrial dysfunction, and inflammasome signaling. Thus, albumin dysfunction in SAH appears to represent a continuum, with progressive oxidation further exacerbating an already pathogenic interactome.

Reversibly oxidized HNA1 exhibited a distinct enrichment of inflammatory lipids (leukotriene C4, tetranor-PGE1), mitochondrial stress-associated metabolites (acylcarnitines), immune regulatory proteins (MAP4K1, TACR1, IFNA1), and microbial peptides. These findings are consistent with previous reports linking cysteinylated albumin to endothelial activation, leukocyte adhesion, and oxidative burst (4). The prominent association of HNA1 with bacterial meta-proteins in our cohort supports growing evidence that gut barrier dysfunction and microbial translocation are central drivers of SAH severity (16). Our data suggest that HNA1 may function as a circulating scaffold that concentrates microbial components, thereby facilitating persistent immune activation.

The most striking and clinically relevant findings relate to hyperoxidized HNA2. We demonstrate that HNA2 in SAH non-survivors harbours a uniquely deleterious cargo enriched in inflammatory fatty acids, bile acid–derived metabolites, muramic acid, hypoxia-responsive lipids, innate immune lectins, and stress-adaptive proteins. This profile is highly concordant with known pathophysiological features of severe alcoholic hepatitis, including profound cholestasis, hypoxia, mitochondrial dysfunction, and innate immune hyper-activation (17). Previous clinical studies have shown that HNA2 strongly predicts short-term mortality in cirrhosis (18); however, mechanistic explanations have been lacking. Our data provide a mechanistic basis by showing that HNA2 selectively concentrates molecules that drive arachidonic acid metabolism, TNFR1 signaling, HIF-1 activation, and kynurenine pathway flux pathways previously implicated in immune paralysis, oxidative stress, and poor outcomes in liver failure (2).

A major conceptual advance of this study is the demonstration that oxidized albumin isoforms are tightly coupled to coordinated pathogenic networks rather than random collections of ligands. Strong correlations between HNA1/HNA2 abundance and their associated biomolecules, together with pathway-level enrichment, indicate that albumin oxidation state dictates selective cargo loading. This observation supports a model in which oxidative modifications alter albumin’s binding pockets, thereby reshaping its ligand repertoire (19). Similar phenomena have been described for oxidized lipoproteins in atherosclerosis, where oxidative modifications transform carrier particles into pro-inflammatory entities (20). Our findings extend this paradigm to albumin in liver disease.

By integrating machine learning, ROC analysis, and survival modeling, we identified a concise set of highly pathogenic HNA1 and HNA2 bound bio-molecules with strong prognostic performance. Among these, PPIA emerged as the most powerful predictor of mortality and a biologically compelling therapeutic target. Cyclophilin A has been recognized as a central mediator of inflammation, acting through CD147/CD18 engagement and activation of NFAT, NF-κB, and MAPK pathways (9). Elevated circulating PPIA levels have been reported in sepsis, acute lung injury, and cardiovascular disease, where they correlate with disease severity and mortality (21) (22). Our study is the first to demonstrate that PPIA is preferentially carried by HNA2 in SAH non-survivors, suggesting that albumin serves as a delivery platform that concentrates and potentially stabilizes this potent inflammatory mediator.

Functional validation using primary human neutrophils provides strong causal support for this concept. We show that SAH-derived HNA2 directly induces neutrophil activation, degranulation, migration,

oxidative burst, and pro-inflammatory cytokine production, closely mimicking PMA stimulation. Importantly, pharmacological inhibition of PPIA with cyclosporin A reverses these effects at both phenotypic and proteomic levels, restoring antioxidant and anti-inflammatory programs. These findings align with prior reports that cyclosporin A and other cyclophilin inhibitors attenuate inflammatory signaling and tissue injury in experimental models of sepsis and ischemia-reperfusion (23). Our data extend these observations to SAH and provide a mechanistic rationale for targeting PPIA in this context.

The therapeutic implications of our findings are substantial. Albumin infusion is widely used in cirrhosis and SAH, primarily to improve oncotic pressure and circulatory function (24). However, recent trials have produced mixed results, suggesting that simply increasing albumin quantity may be insufficient (25). Our data suggest that the qualitative composition of albumin specifically the balance between reduced and oxidized isoforms and their associated cargo may be equally important. Strategies aimed at “albumin detoxification,” such as displacement of pathogenic ligands, or pharmacological targeting of key HNA2-bound mediators such as PPIA, could represent a new therapeutic paradigm. Extracorporeal albumin dialysis systems and adsorption columns have already shown promise in removing protein-bound toxins in liver failure; isoform-selective approaches may further enhance efficacy (26).

Several limitations should be acknowledged. Although our cohorts were well characterized and adequately powered, external validation in independent populations will be important. Our in-vitro studies focused on neutrophils; future work should examine effects on other immune and parenchymal cells, including monocytes, macrophages, and hepatocytes. Finally, while cyclosporin A effectively inhibited PPIA-dependent signaling in vitro, its immunosuppressive properties necessitate careful evaluation in the context of SAH, where infection risk is high. Development of more selective cyclophilin inhibitors may provide safer alternatives.

In conclusion, this study reveals that oxidized albumin isoforms in SAH are active pathogenic entities that orchestrate inflammatory and oxidative networks through selective cargo binding. HNA2, in particular, serves as a carrier for highly deleterious biomolecules, including PPIA, and directly drives neutrophil-mediated inflammation. These findings redefine albumin from a passive biomarker to a central mechanistic hub in SAH pathogenesis and nominate the HNA2–PPIA axis as a promising therapeutic target.

Abbreviations

UHPLC	Ultra-High-Performance Liquid Chromatography
HRMS	High Resolution Mass Spectrometry
HMA	Human Mercaptoalbumin
HNA1	Human Nonmercaptoalbumin 1
HNA2	Human Nonmercaptoalbumin 2

DC	Decompensated Cirrhosis
SAH	Severe Alcoholic Hepatitis
ROS	Reactive oxygen species
PPIA	Peptidylprolyl isomerase A
SPPL2B	Ssignal peptide peptidase like 2B
POD	Probability of Detection
AUC	Area Under Curve
PE	Phosphatidylethanolamine
MELD	Model for End-Stage Liver Disease
ALBI	Albumin-Bilirubin score
PALBI	Platelet-Albumin-Bilirubin score

Declarations

Financial Support*: The work was supported by project* ICMR (IIRP-2023-1575) *and UGC.*

Disclosure: *All authors have declared no conflict of interest.*

Authors' contribution: *JSM conceptualized the work. BM was responsible for sample processing and experimental work with the help of SP, VB, GT, VS, NS, NS, MY and SY. Data analysis was performed by BM and SP under the guidance of JSM. The manuscript was drafted by BM and JSM. SS provided critical feedback. Senior Professor Shiv Kumar Sarin provided critical inputs to the manuscript. All authors have approved this manuscript.*

References

1. Ha Y, Jeong I, Kim TH. Alcohol-Related Liver Disease: An Overview on Pathophysiology, Diagnosis and Therapeutic Perspectives. Biomedicines. 2022;10(10).
2. Sharma N, Pandey S, Yadav M, Mathew B, Bindal V, Sharma N, et al. Biomolecular map of albumin identifies signatures of severity and early mortality in acute liver failure. J Hepatol. 2023;79(3):677–91.
3. Casulleras M, Flores-Costa R, Duran-Guell M, Zhang IW, Lopez-Vicario C, Curto A, et al. Albumin Lipidomics Reveals Meaningful Compositional Changes in Advanced Cirrhosis and Its Potential to Promote Inflammation Resolution. Hepatol Commun. 2022;6(6):1443–56.

4. Alcaraz-Quiles J, Casulleras M, Oettl K, Titos E, Flores-Costa R, Duran-Guell M, et al. Oxidized Albumin Triggers a Cytokine Storm in Leukocytes Through P38 Mitogen-Activated Protein Kinase: Role in Systemic Inflammation in Decompensated Cirrhosis. Hepatology. 2018;68(5):1937–52.
5. Bhat A, Das S, Yadav G, Chaudhary S, Vyas A, Islam M, et al. Hyperoxidized Albumin Modulates Platelets and Promotes Inflammation Through CD36 Receptor in Severe Alcoholic Hepatitis. Hepatol Commun. 2020;4(1):50–65.
6. Paar M, Cvirn G, Hoerl G, Reibnegger G, Sourij H, Sourij C, et al. Albumin of People with Diabetes Mellitus Is More Reduced at Low HbA1c. Int J Mol Sci. 2023;24(22).
7. Das S, Maras JS, Hussain MS, Sharma S, David P, Sukriti S, et al. Hyperoxidized albumin modulates neutrophils to induce oxidative stress and inflammation in severe alcoholic hepatitis. Hepatology. 2017;65(2):631–46.
8. Das S, Hussain MS, Maras JS, Kumar J, Shasthry SM, Nayak S, et al. Modification Patterns of Urinary Albumin Correlates With Serum Albumin and Outcome in Severe Alcoholic Hepatitis. J Clin Gastroenterol. 2019;53(6):e243-e52.
9. Bai X, Yang W, Zhao Y, Cao T, Lin R, Jiao P, et al. The extracellular cyclophilin A-integrin beta2 complex as a therapeutic target of viral pneumonia. Mol Ther. 2024;32(5):1510–25.
10. Narro GEC, Diaz LA, Ortega EK, Garin MFB, Reyes EC, Delfin PSM, et al. Alcohol-related liver disease: A global perspective. Ann Hepatol. 2024 Sep-Oct;29(5):101499.
11. Pompili E, Zaccherini G, Piano S, Toniutto P, Lombardo A, Gioia S, et al. Real-world experience with long-term albumin in patients with cirrhosis and ascites. JHEP Rep. 2024;6(12):101221.
12. Oettl K, Marsche G. Redox state of human serum albumin in terms of cysteine-34 in health and disease. Methods Enzymol. 2010;474:181–95.
13. Belinskaia DA, Jenkins RO, Goncharov NV. Serum Albumin in Health and Disease: From Comparative Biochemistry to Translational Medicine. Int J Mol Sci. 2023;24(18).
14. Longo LV, Nakayasu ES, Matsuo AL, Peres da Silva R, Sobreira TJ, Vallejo MC, et al. Identification of human plasma proteins associated with the cell wall of the pathogenic fungus Paracoccidioides brasiliensis. FEMS Microbiol Lett. 2013;341(2):87–95.
15. Oettl K, Stauber RE. Physiological and pathological changes in the redox state of human serum albumin critically influence its binding properties. Br J Pharmacol. 2007;151(5):580–90.
16. Raya Tonetti F, Eguileor A, Mrdjen M, Pathak V, Travers J, Nagy LE, et al. Gut-liver axis: Recent concepts in pathophysiology in alcohol-associated liver disease. Hepatology. 2024;80(6):1342–71.
17. Bataller R, Arab JP, Shah VH. Alcohol-Associated Hepatitis. N Engl J Med. 2022;387(26):2436–48.
18. Bernardi M, Angeli P, Claria J, Moreau R, Gines P, Jalan R, et al. Albumin in decompensated cirrhosis: new concepts and perspectives. Gut. 2020;69(6):1127–38.
19. Oettl K, Birner-Gruenberger R, Spindelboeck W, Stueger HP, Dorn L, Stadlbauer V, et al. Oxidative albumin damage in chronic liver failure: relation to albumin binding capacity, liver dysfunction and survival. J Hepatol. 2013;59(5):978–83.

20. Poznyak AV, Nikiforov NG, Markin AM, Kashirskikh DA, Myasoedova VA, Gerasimova EV, et al. Overview of OxLDL and Its Impact on Cardiovascular Health: Focus on Atherosclerosis. Front Pharmacol. 2020;11:613780.
21. Ohtsuki T, Satoh K, Omura J, Kikuchi N, Satoh T, Kurosawa R, et al. Prognostic Impacts of Plasma Levels of Cyclophilin A in Patients With Coronary Artery Disease. Arterioscler Thromb Vasc Biol. 2017;37(4):685–93.
22. Tegeder I, Schumacher A, John S, Geiger H, Geisslinger G, Bang H, et al. Elevated serum cyclophilin levels in patients with severe sepsis. J Clin Immunol. 1997;17(5):380–6.
23. Stauffer WT, Goodman AZ, Gallay PA. Cyclophilin inhibition as a strategy for the treatment of human disease. Front Pharmacol. 2024;15:1417945.
24. Pares A, Deulofeu R, Cisneros L, Escorsell A, Salmeron JM, Caballeria J, et al. Albumin dialysis improves hepatic encephalopathy and decreases circulating phenolic aromatic amino acids in patients with alcoholic hepatitis and severe liver failure. Crit Care. 2009;13(1):R8.
25. China L, Freemantle N, Forrest E, Kallis Y, Ryder SD, Wright G, et al. A Randomized Trial of Albumin Infusions in Hospitalized Patients with Cirrhosis. N Engl J Med. 2021;384(9):808–17.
26. Agarwal B, Canizares RB, Saliba F, Ballester MP, Tomescu DR, Martin D, et al. Randomized, controlled clinical trial of the DIALIVE liver dialysis device versus standard of care in patients with acute-on-chronic liver failure. J Hepatol. 2023;79(1):79–92.

Figures

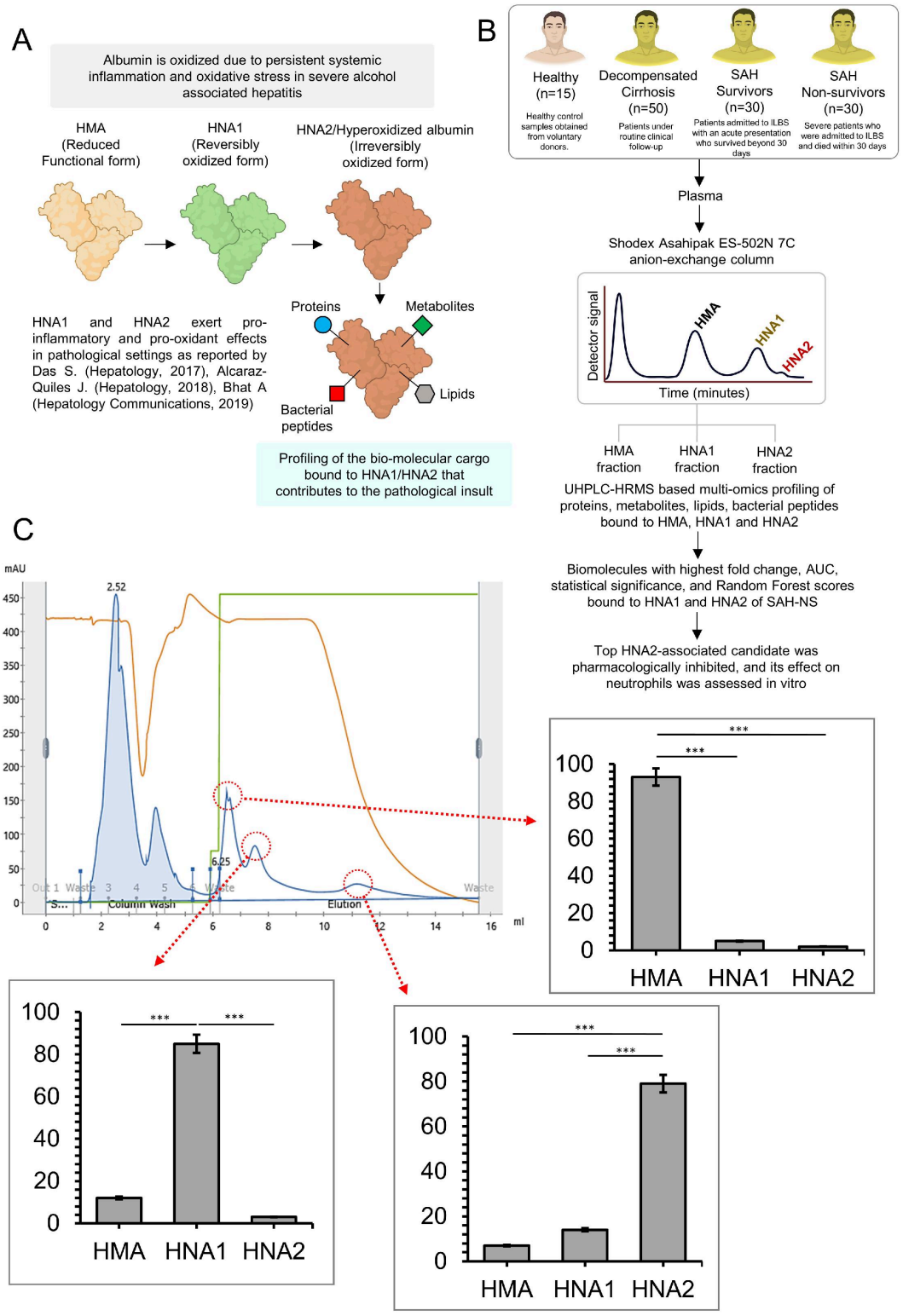


Figure 1

Oxidative stress driven remodeling of albumin redox isoforms and study workflow in severe alcohol-associated hepatitis (SAH).

(A) Schematic depicting progressive oxidation of human mercaptalbumin (HMA) to reversibly oxidized HNA1 (cysteinylated/homocysteinylated at Cys-34) and irreversibly hyperoxidized HNA2

(sulfinic/sulfonic acid derivatives), and their proposed pathogenic roles in SAH.

(B) Overall study design: plasma samples from healthy controls, decompensated cirrhosis, SAH survivors, and SAH non-survivors were fractionated by anion-exchange chromatography into HMA, HNA1, and HNA2, followed by UHPLC-HRMS based multi-omics profiling to identify isoform-specific bound biomolecules; top HNA2-associated candidate was pharmacologically inhibited and functionally validated in neutrophil assays.

(C) Representative chromatograms and top-down proteomics confirming reproducible separation, identity, and purity of HMA, HNA1, and HNA2 fractions.

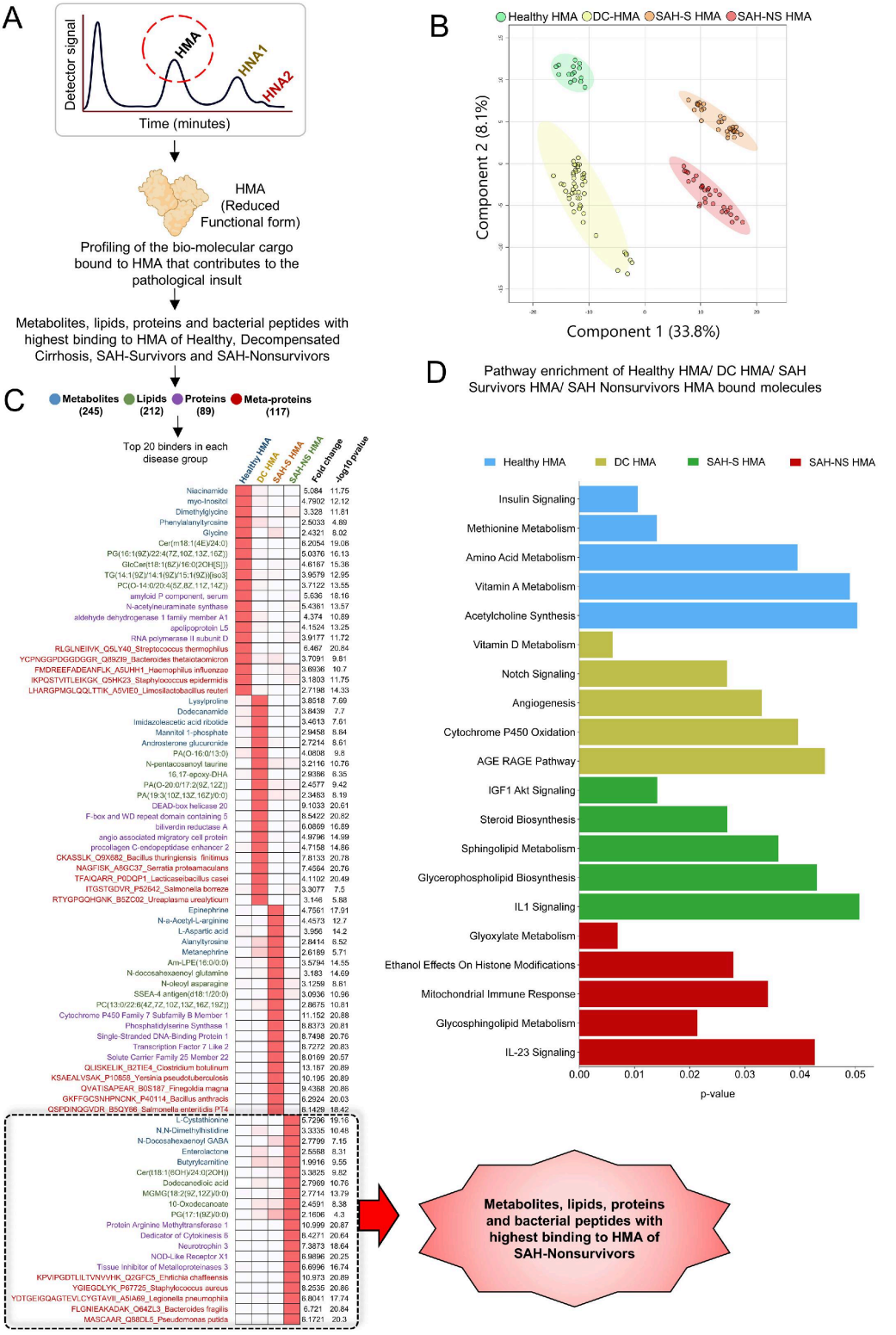


Figure 2

Bio-molecular cargo linked to HMA in severe alcohol-associated hepatitis.

(A) Workflow depicting isolation of HMA by anion-exchange chromatography and UHPLC-HRMS based multi-omics profiling of bound metabolites, lipids, host proteins, and bacterial peptides across study cohorts.

(B) Principal component analysis of integrated HMA bound multi-omics features across healthy controls, decompensated cirrhosis, SAH survivors, and SAH non-survivors.

(C) Heatmap showing top discriminatory HMA bound biomolecules selected based on fold change and statistical significance.

(D) Pathway enrichment analysis of HMA associated biomolecules identified from multi-omics profiling.

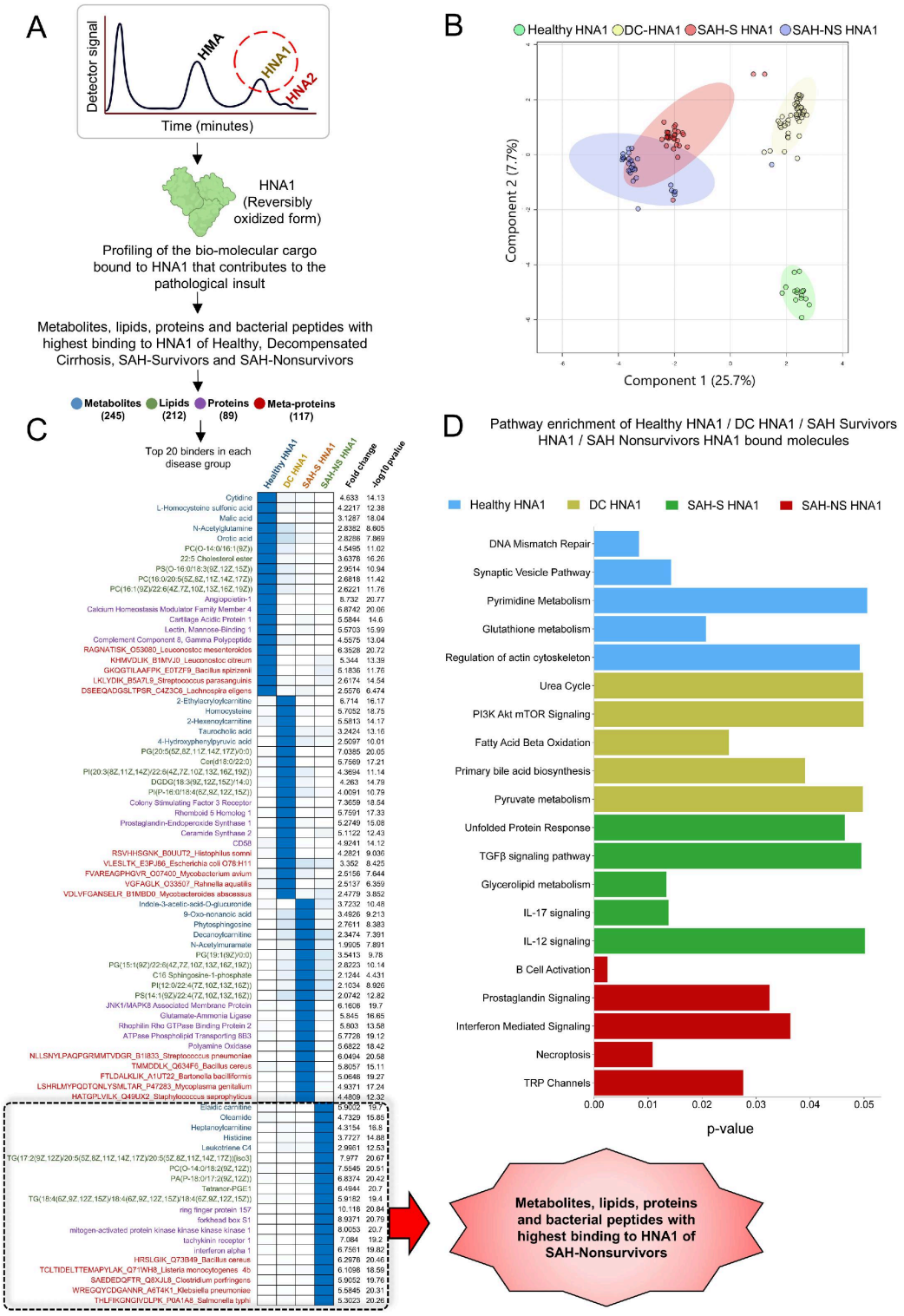


Figure 3

Bio-molecular cargo associated with HNA1 in severe alcohol-associated hepatitis.

(A) Schematic of HNA1 isolation by anion-exchange chromatography followed by UHPLC-HRMS based multi-omics characterization of bound metabolites, lipids, host proteins, and bacterial peptides across study cohorts.

(B) Principal component analysis of integrated HNA1 bound multi-omics features from healthy controls, decompensated cirrhosis, SAH survivors, and SAH non-survivors.

(C) Heatmap depicting top discriminatory HNA1-associated biomolecules selected based on fold change and statistical significance.

(D) Pathway enrichment analysis of HNA1-bound biomolecules derived from multi-omics profiling.

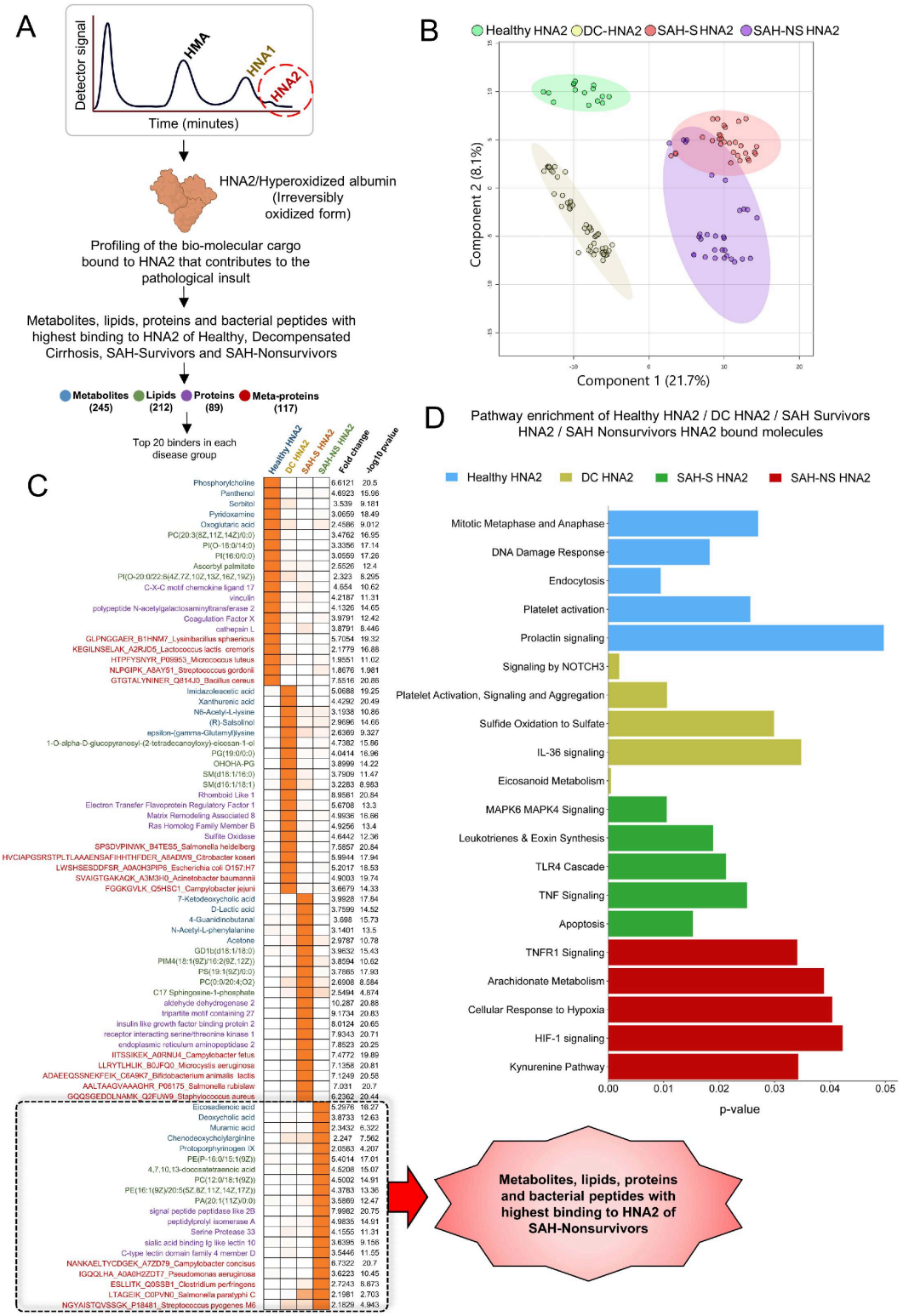


Figure 4

Pathological remodeling of the biomolecular cargo bound to HNA2 in severe alcohol-associated hepatitis.

(A) Workflow illustrating HNA2 isolation by anion-exchange chromatography and subsequent UHPLC-HRMS based multi-omics profiling of bound metabolites, lipids, host proteins, and bacterial peptides

across study cohorts.

(B) Principal component analysis of integrated HNA2 bound multi-omics features from healthy controls, decompensated cirrhosis, SAH survivors, and SAH non-survivors.

(C) Heatmap showing top discriminatory HNA2 associated bio-molecules selected based on fold change and statistical significance.

(D) Pathway enrichment analysis of HNA2 bound biomolecules identified through multi-omics profiling.

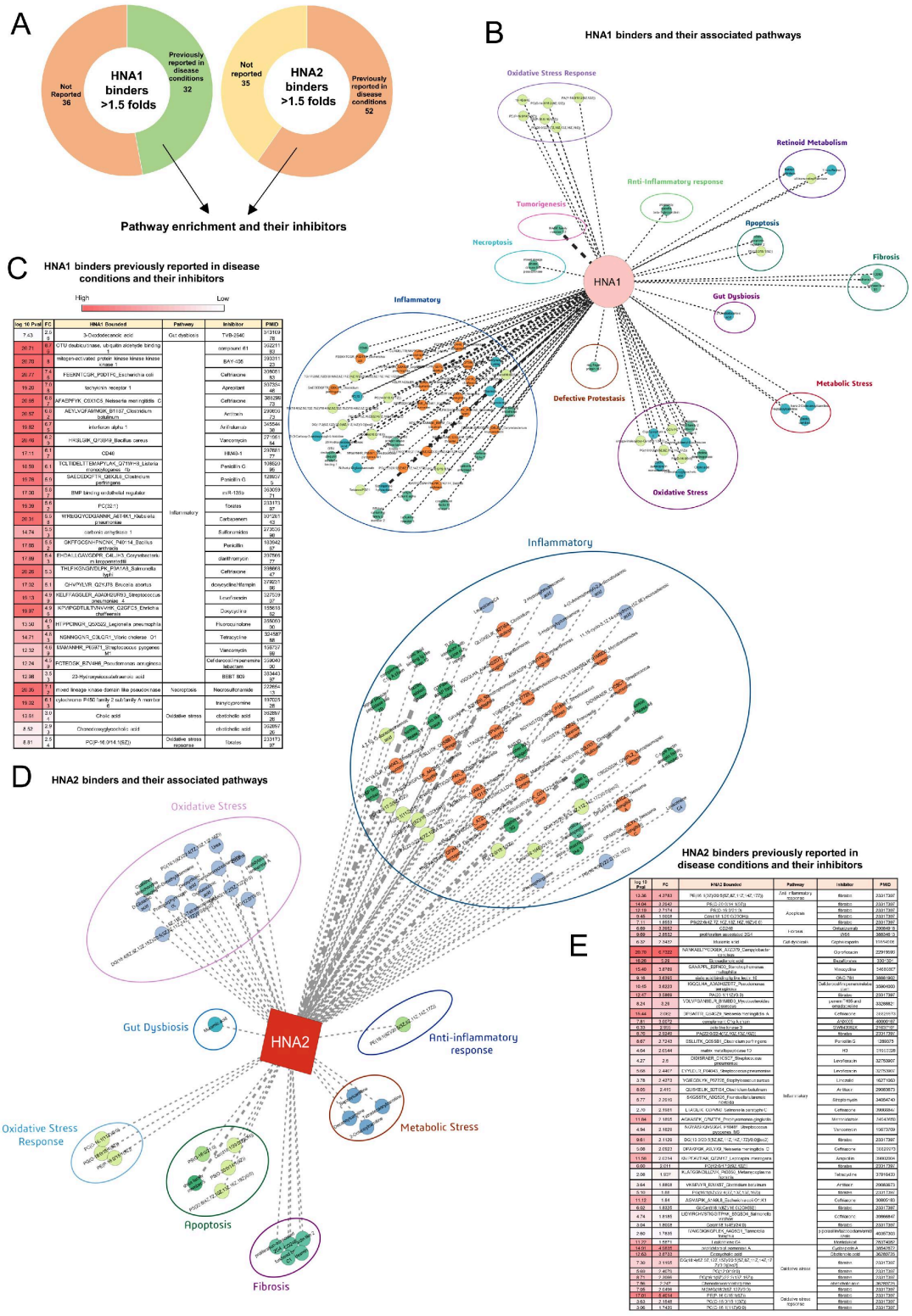


Figure 5

HNA1 and HNA2 associate with therapeutically tractable bio-molecular networks in severe alcohol-associated hepatitis.

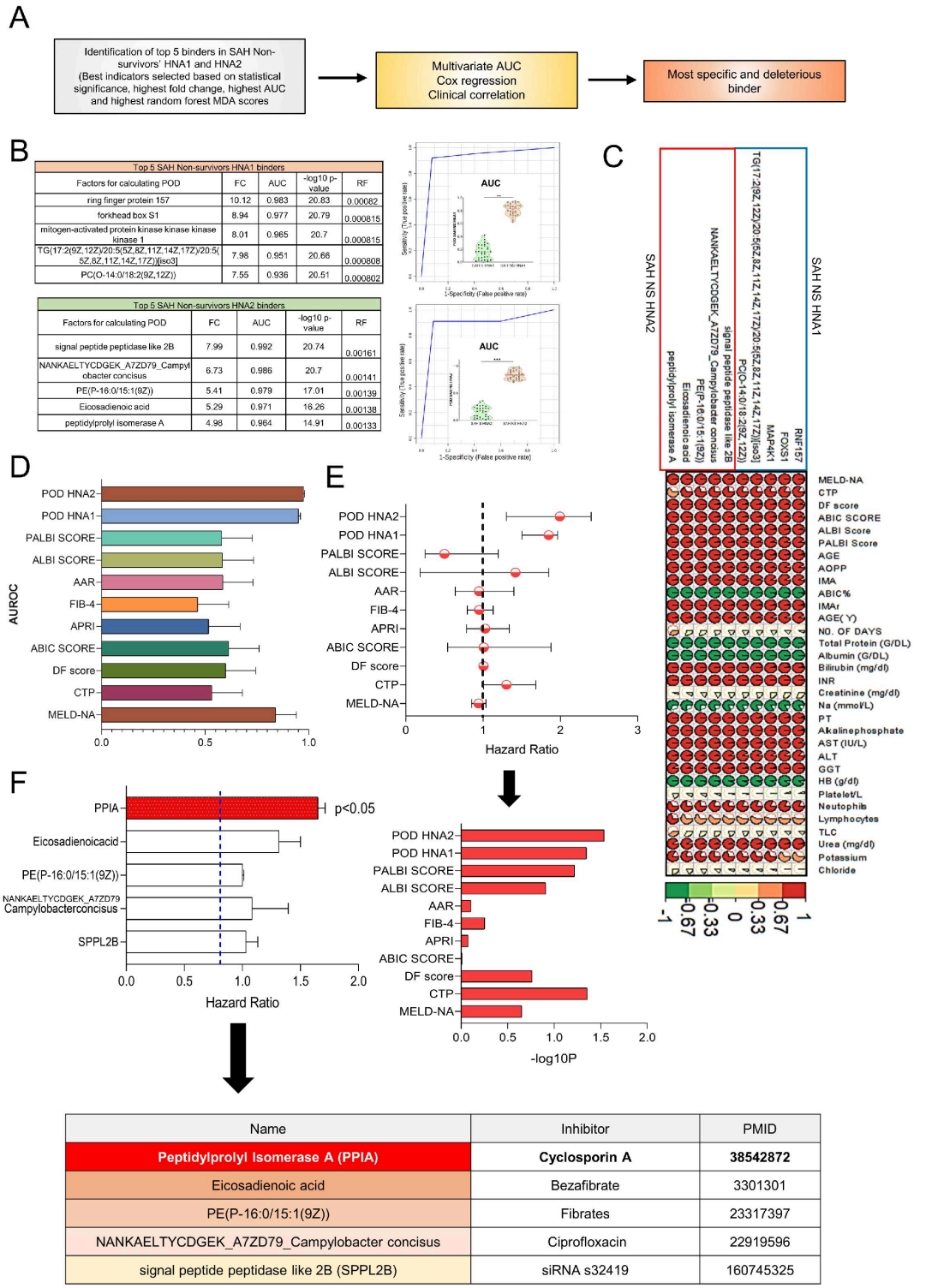
(A) Overview of significantly enriched bio-molecules associated with HNA1 and HNA2 in SAH non-survivors identified using stringent fold-change and statistical significance thresholds.

(B) Functional correlation network map of HNA1 bound bio-molecules grouped into major biological and pathological pathway categories.

(C) Drug target network depicting known pharmacological inhibitors and clinically relevant compounds mapped to HNA1 associated biomolecules.

(D) Functional correlation network map of HNA2 associated biomolecules grouped into major biological and pathological pathway categories.

(E) Drug target network illustrating known pharmacological inhibitors and therapeutic agents mapped to HNA2 associated biomolecules.



Name	Inhibitor	PMID
Peptidylprolyl Isomerase A (PPIA)	**Cyclosporin A**	**38542872**
Eicosadienoic acid	Bezafibrate	3301301
PE(P-16:0/15:1(9Z))	Fibrates	23317397
NANKAELTYCDGEK_A7ZD79_Campylobacter concisus	Ciprofloxacin	22919596
signal peptide peptidase like 2B (SPPL2B)	siRNA s32419	160745325

Figure 6

Integrated machine-learning and survival modelling identifies a core set of pathogenic HNA1 and HNA2 bound bio-molecules in severe alcohol-associated hepatitis.

(A) Schematic workflow of the multi-layered biomarker prioritization pipeline integrating fold change, statistical significance, AUROC, Random Forest importance, multivariate modelling, Cox regression, and

clinical correlations.

(B) Table depicting fold change, AUC, -log 10 p-value, MDA and Probability of detection value of top-ranked HNA1 and HNA2 associated biomolecules.

(C) Heatmap depicting correlations between prioritized biomolecules and clinical indices of SAH disease severity, albumin modification markers, and laboratory parameters.

(D) Comparative AUROC graph of POD of HNA1 and HNA2 associated bio-molecules and SAH severity scores.

(E) Forest plot of Cox proportional hazards regression showing associations between prioritized biomolecules and 30-day mortality.

(F) Hazard ratio plot and Drug target table highlighting pharmacological tractability of the top HNA2-associated candidate.

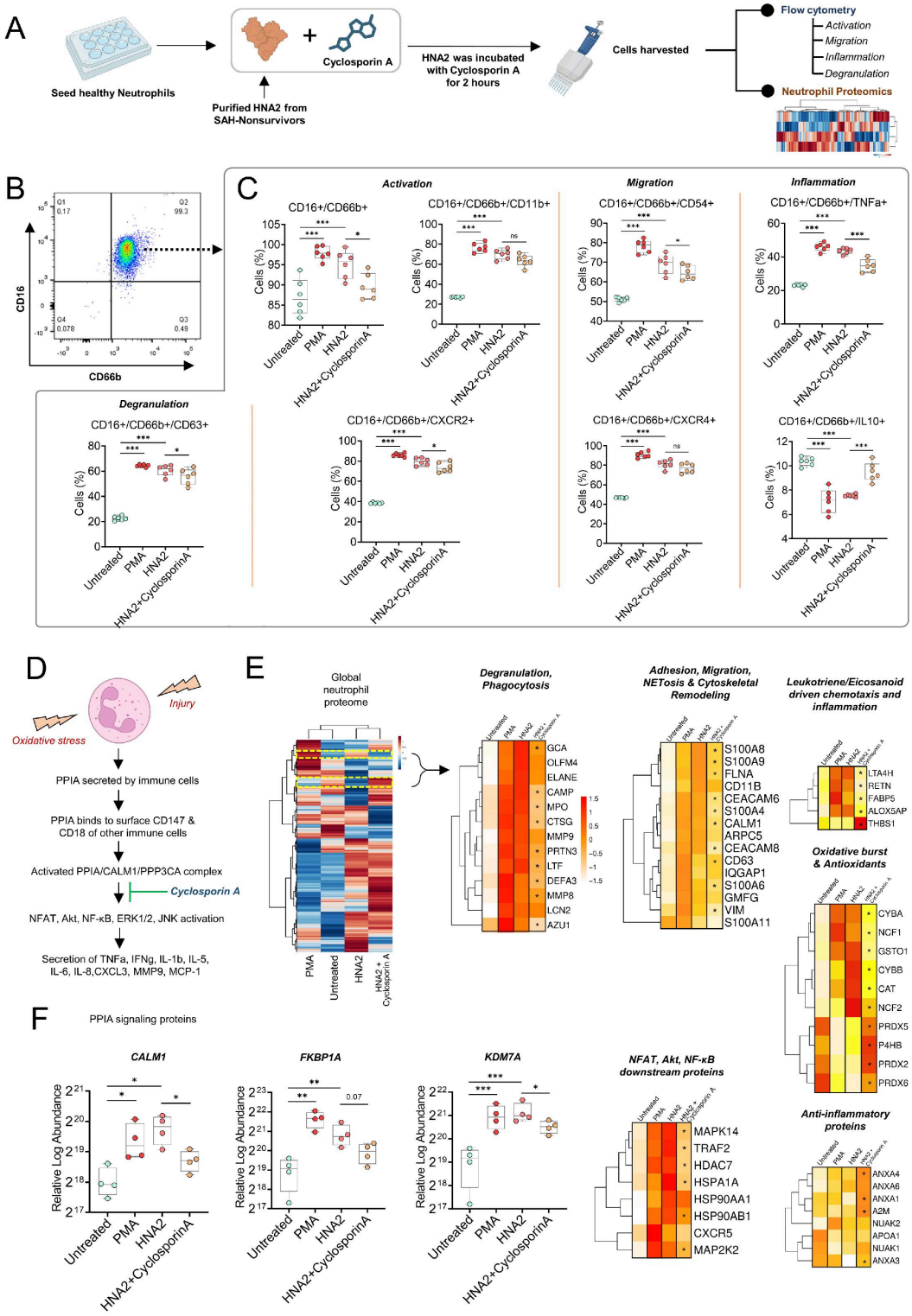


Figure 7

HNA2 induces a PPIA-dependent pro-inflammatory and pro-oxidant activation program in primary human neutrophils that is reversed by Cyclosporin A.

(A) Experimental workflow depicting treatment of primary human neutrophils with SAH derived HNA2, PMA, or SAH-derived HNA2 plus Cyclosporin A, followed by multi-parametric flow cytometry and global

proteomic profiling.

(B) Representative flow cytometry gating plot of for identification of neutrophil activation ($CD16^{+}CD66b^{+}$).

(C) Flow cytometry quantification of neutrophil activation, migration, degranulation, adhesion/migration, inflammatory, and anti-inflammatory populations across treatment conditions.

(D) Schematic flow of PPIA-mediated signaling cascades and downstream inflammatory pathways in neutrophils.

(E) Heatmap of differentially regulated neutrophil proteins involved in degranulation, phagocytosis, adhesion, migration, NETosis/cytoskeletal remodeling, eicosanoid signaling, oxidative burst, antioxidant defense, and anti-inflammatory responses.

(F) Heatmap of PPIA-associated downstream signaling proteins modulated across treatment conditions.

Supplementary Files

This is a list of supplementary files associated with this preprint. Click to download.

- SupplementaryMethods18022026.docx
- GraphicalAbstract.pdf
- SupplementaryFiguresXTables18022026.docx